RESEARCH ARTICLE

A tandem of GC-MS and electroanalysis for a rapid chemical profiling of bacterial extracellular matrix

Y. E. Silina[1, 2] | E. V. Zolotukhina[3] | M. Koch[4] | C. Fink-Straube[4]

[1]Institute of Biochemistry, Saarland University, Saarbrücken, Germany

[2]KIST – Korea Institute of Science and Technology, Europe Forschungsgesellschaft, Saarbrücken, Saarbrücken, Germany

[3]Federal Research Center of Problems of Chemical Physics and Medicinal Chemistry, Russian Academy of Sciences, Moscow region, Russia

[4]INM – Leibniz Institute for New Materials, Saarbrücken, Germany

Correspondence
Y. E. Silina, Institute of Biochemistry, Saarland University, Campus B 2.2, room 317, 66123, 66123 Saarbrücken, Germany.
Email: yuliya.silina@gmx.de and yuliya.silina@uni-saarland.de

Abstract

Herein an assay toward a rapid and reliable profiling of extracellular matrix of *Escherichia coli (E. coli)* utilizing a tandem of GC-MS as a tool for definition of the exact chemical nature of low molecular weight compounds and cyclic voltammetry for their high throughput detection is presented.

Briefly, during a set of investigations the formation of glycerol in the extracellular matrix (ECM) of *E. coli* at physiological relevant conditions of cells was revealed. Based on the obtained knowledge, the electrochemical protocol allowing both qualitative and quantitative analyses of glycerol in *E. coli* ECMs at palladium ink-modified screen printed electrodes with precision values (RSD) $< 10\%$ and recovery rates ranged from 98% to 102% was proposed.

The provided protocol for a rapid electrochemical profiling of the bacterial ECMs can readily be used as a guideline for the controlled electroanalysis of target electroactive signaling analytes in complex biological samples.

KEYWORDS
cyclic voltammetry, *E. coli* extracellular matrix, electrochemical profiling, Pd-ink-modified electrode

1 | INTRODUCTION

Escherichia coli (*E. coli*) cells have a complex extracellular matrix (ECM) consisting of the protein polymer named curli and the polysaccharide cellulose [1]. Although several studies reporting ECM structure and techniques that can be used for its analysis were published [1–3], the extracellular content of *E. coli* ECM represented by low molecular weight compounds remains not well understood.

For profiling of *E. coli* ECM based on small peptides composition and their ratio a tandem mass spectrometry (MS/MS) is mostly being utilized [4]. However, almost no attempts were conducted towards the definition of *E. coli* ECM compounds with a molecular weight below ≤ 1 kDa. Meanwhile, during fermentation pathways *E. coli* can produce a mixture of non-protein low molecular weight compounds released in ECM [5, 6]. For example, as a result of bacterial activity the formation of carbon disulfide, butanal, indole, isoprene,

dextrose cadaverine, octanol, propanol, butanol, 2-ethyl-1-hexanol and 2,5-dimethyl-pyrazine in ECM of *E. coli* detected by gas chromatography mass spectrometry (GC-MS) was reported [6, 7]. At the same time, low molecular weight compounds produced or formed as secondary metabolites serve as signaling biomarkers and, thus, can readily be used for a chemical profiling of bacterial cells.

However, utilizing GC-MS alone it is almost impossible to reach a high throughput analysis of the samples assembly. In the majority GC-MS assays applied for the analysis of real biological samples require an essential sample preparation procedure and a separation of mixtures into the individual compounds [8–10]. The data acquisition is quite complex, time consuming and requires highly educated and experienced personal.

As an alternative to GC-MS, electrochemical methods (*i.e.* cyclic voltammetry, CV, amperometry, AM, etc.) provide a good basis for a rapid and simple samples profiling with a high sensitivity and resolution. Thus, electroanalysis of alcohols can be carried out during only several minutes at the surface of Pd, Rh or PdRh catalysts [11, 12]. Selective and sensitive electrodetection of acetaldehyde and formaldehyde can be implemented in basic aqueous solutions by use of Ag and Pd nanoparticles-based electrocatalysts [13, 14]. The detection of carbohydrates at basic pH on nanostructured electrodes at low applied potentials also appears to be possible [15–17]. As a disadvantage, it is worth noting that the electrochemical methods do not allow establishing the exact chemical nature of electroactive compounds responsible/causing the signal formation in complex media, *i.e.* fermentation samples.

Here an assay towards a rapid and reliable profiling of extracellular matrix of *Escherichia coli (E. coli)* utilizing a tandem of GC-MS as a tool for definition of the exact chemical nature of electroactive low molecular weight compound and cyclic voltammetry for its high throughput detection is presented.

The novelty of this study relies on the detection scheme coupled with a chromatography step for *E. coli ECM* analysis and control (*i*), revealing the chemical nature of electroactive compound formed in *E. coli* ECM as result of bacterial activity (*ii*), definition of electrochemical conditions towards detection of the established electroactive compound in complex fermentation media (*iii*) and *in vitro* non-enzymatic profiling of *E. coli* ECM utilizing Pd-ink modified microelectrodes (*iv*).

It is believed that the proposed approach represents a significant advance in our understanding of *E. coli* extracellular matrix nature and its potential as a source of electroactive compounds for non-invasive *in vitro* profiling using electrochemical techniques.

2 | EXPERIMENTAL PART

2.1 | Materials and methods

The DRP-110PDP screen printed electrodes (SPEs) covered by palladium ink (Pd-ink) were obtained from DropSens (Metrohm, Germany, Filderstadt). *Escherichia coli* C43(DE3), genotype F – ompThsdSB (rB- mB−) gal dcm (DE3) was obtained from Lucigen (USA, Wisconsin). Cultivation M9 medium, glucose, soluble starch, derivatization agent N-Trimethylsilyl-N-methyl trifluoroacetamide (MSTFA), $CoCl_2$ (98%) and 30% H_2O_2 were obtained from Merck (Germany, Darmstadt).

2.2 | *E. coli* cultivation for the chemical and electrochemical profiling

E. coli cells were cultivated in M9 medium (6 g/L Na_2HPO_4, 3 g/L KH_2PO_4, 0.5 g/L NaCl, 1 g/L NH_4Cl, 2 g/L casamino acids in 1 L of DI water) supported by 2% glucose or 2% of soluble starch. The use of soluble starch as a carbon source for *E. coli* growth was described in several studies [18–20]. Regardless of the carbon source used, cells were cultivated at 37 °C at a shaking rate of 160 rpm for 24 h (unless otherwise specified). The optical density (OD) of cells was determined by DiluPhotometer™ OD600 mini-spectrophotometer at 600 nm (Implen GmbH, Munich, Germany). Further, the cells were removed from the cultivation medium by centrifugation conducted at 5000 rpm for 10 min. The received *E. coli* extracellular matrix (will be further referred as ECM) were used for the subsequent investigations.

E. coli ECMs obtained from cells grown under various test-conditions were referred as follows: cells with an OD 3.7 grown in 2% glucose-supported M9 medium (sample I), cells with the OD 4.1 grown in 2% glucose-supported M9 medium with addition of 1 mM of $CoCl_2$ (sample II); cells with the OD 3.9 grown in 2% glucose-supported M9 medium with addition of 1 mM of H_2O_2 (sample III); cells with the OD 6.3 grown in 2% starch-supported M9 medium (sample IV).

2.3 | Electrochemical screening of *E. coli* ECM

The electrochemical profiling of *E. coli* ECM samples was carried out on commercial three-electrode SPEs with the working electrode modified by Pd-ink (DropSens, Metrohm, Germany). The analytical performance of these electrodes was tested in a droplet (150 μL of the

test solution was applied) of working solutions (buffer, DI water, cultural media, ECM of *E. coli*) using CV mode at 20 mV/s (unless otherwise specified) in a potential window from −0.4 V to 0.8 V *vs.* silver chloride electrode. The pH of working solutions were ranged from physiological (~6–7) to 12 via addition of KOH pellets (pH control via pH meter). Testing of glycerol was also carried out in buffered and cultural media solutions at various pH. Regardless of the sample type or model solutions all experiments scans were performed at least in triplicate. Data acquisition was conducted for the second scan (unless otherwise specified) and presented with ± SD.

2.4 | Scanning electron microscopy (SEM)

The modified by Pd-ink SPEs were investigated by SEM-EDX using an FEI Quanta 400 FEG. The electrodes were placed on the sample stage and electrically connected to the stage using double sided carbon tape. Secondary (SE) and Back scattered (BSE) electron images were acquired in high vacuum mode at 10 kV accelerating voltage. X-ray spectral analysis was performed using an EDAX Genesis V6.04 spectrometer.

2.5 | FT-IR studies

FT-IR analysis of a dried droplet of *E. coli* ECM was performed on a FT-IR spectrometer IRSpirit (Shimadzu, Tokyo). For the data acquisition Lab Solutions IR software (Shimadzu, Tokyo) was utilized. To verify the presence of glycerol in a model/standard or fermentation medium, the following characteristic bounds were monitored: 2931, 2877, 1425, 1327, 1210, 1107, 1027, 992, 920, 851 cm^{-1} [21, 22].

To screen the surface chemistry of Pd-ink modified electrode, the functional layer was scratched from the surface of SPEs for the subsequent FT-IR analysis.

2.6 | GC-MS chemical profiling

For the control of the chemical nature of low molecular weight compounds formed in *E. coli* ECM depending on the carbon source used, the following GC-MS protocols were applied. First, the intact samples were investigated as they are (without any sample pre-concentration or derivatization procedure) on a GC/MS QP2010 (Shimadzu). The separation of ECM mixture was conducted on a DB-HeavyWax (30 m, 0.25 mm, 0.25 μm) column at start temperature of 50 °C/min, followed by a temperature increase to 20 K/min, 200 °C/3 min and finally to 50 K/min 250 °C for 5 min. The injection temperature was set to 50 °C, split ratio 1 to 5; column flow was adjusted at 1 mL/min. This protocol was referred to *approach 1.*

For comparison of the results obtained by *approach 1*, the aqueous phase was evaporated from the intact 200 μL of ECM samples under N$_2$-atmosphere followed by the subsequent derivatization step. For this goal, to the obtained dried extract 40 μL of a MSTFA reagent was added. The suspension was heated at 60 °C for 30 min [23]. Finally, 1 μL of the received sample was injected into the GC-MS system. In this case the chromatographic analysis was performed on a TSQ-9000 Trace 1310 (Triple quadrupole MS, Thermo Fisher Scientific), equipped with an autosampler (Thermo TriPlus). GC-MS separation of the obtained samples was carried out on a MXT column (cross-bond 100 % dimethyl polysiloxane, 0.25 mm×30 m×0.25 μm thickness, PESTEK) in a splitless mode and a purge flow of 5 mL/min at the following gradient conditions: starting temperature was 100 °C held for 2 min, raised to 220 °C at 20 °C/min for 7 min and held at 300 °C for 13 min. The analysis of *E. coli* ECMs performed according to this procedure was referred to *approach 2.*

Regardless of the approach mass spectra were recorded in both TIC and EIC modes in the range of *m/z* 100–500. MS transfer line temperature was 280 °C, ion source temperature 220 °C.

3 | RESULTS AND DISCUSSION

3.1 | Electrochemical aspects of *E. coli* ECM profiling

In our previous study the possibility for a rapid electrochemical profiling of yeast ECM (y-ECM) conducted *in vitro* during only several minutes at low scan rates and physiological conditions of cells utilizing screen printed electrodes (SPEs) was demonstrated [24]. By tuning of electrochemical conditions it was possible to adjust the electrochemical profiling of y-ECM.

Herein, the electroanalytical performance of the commercial Pd-ink modified SPE was explored in ECM of *E. coli.* The surface of the working electrode consisted of spherical Pd-nanoparticle agglomerates in the sub-micron range (~600–800 nm) surrounded by a thin polymer layer, see ESI, Figure S1A. EDX analysis of the electrode surface revealed the presence of Pd, C and O in the spectra as the main components of the functional electroactive layer, ESI, Figure S1B. The organic binding component was most likely represented by polyacrylamide

(see FT-IR profile recorded from Pd-ink in comparison with FT-IR spectra obtained for polyacrylamide used as a standard sample, ESI, Figure S1C).

In contrast to the dependencies seen during analysis of y-ECM, CV plots recorded from the surface of these SPEs in droplets of all tested intact *E. coli* ECMs were almost identical regardless of the used scan rates (data not shown). Hence, at these conditions no electrochemical profiling of samples by means of the previously optimized y-ECM approach was possible ESI, Figure S2.

This result can be explained either *(i)* by the absence of electroactive compounds in *E. coli* ECMs which could be oxidized on Pd-ink modified SPEs at the used experimental conditions or *(ii)* by the presence of electrochemically inactive compounds in solution adsorbed on the surface of the working electrode but inactivated. Alternatively, *(iii)* the used experimental conditions were not optimal for electrodetection of any electroactive analytes in ECMs on Pd-ink modified electrodes.

Keeping in mind that in analyzed solutions at least residual medium compounds (*i.e.* amino acids, sugars, etc.) remaining in ECMs at different amounts depending on the growth conditions or formed novel electroactive metabolites should be present, the aspects *(ii)* and *(iii)* appear to be more reasonable. In other words, first, the nature of electroactive compounds present in ECMs should be determined (see next sections).

3.2 | GC-MS analysis of *E. coli* ECM

To clarify the chemical composition of tested ECM samples, a GC-MS study was contacted firstly by *approach 1*. Unfortunately, a poor spectrum of low molecular weight organic compounds formed in tested ECMs was obtained: apart from acetic acid, methyl carbamate and 5-methylfurfural no other molecular species were detected, ESI, Figure S3, S4. More importantly, regardless of the sample type and cultivation conditions used the same chromatographic profile was obtained for tested ECMs that makes their chemical profiling by means of *approach 1* impossible.

In attempts to discover/"open" the truly content of *E. coli* ECM represented by low molecular weight compounds, next, tested samples were derivatized with MSTFA *prior* to GC-MS analysis (*approach 2*). Interestingly, that chemical profile for all ECMs after derivatization was very rich in terms of the amount of visualized analytes/low molecular weight compounds in the chromatograms, Figure 1.

Thus, the number of peaks with a resolution above 5 and high signal to noise ratio was ranged from 10 to 17 for the tested ECMs samples depending on the conditions used for cells growth (carbon source, chemicals treatment (H_2O_2, $CoCl_2$)). Moreover, the *approach 2* allows obtaining very different chromatograms for various ECMs, and, thus, the conducting of their chemical profiling provided that the characteristic/signaling peak(s) is(are) established. Moreover, the used sample preparation procedure in combination with a GC-MS protocol supports an excellent TIC-profile reproducibility of the results from run-to-run recorded for the same tested sample, ESI, Figure 5 (shown for sample II – ECM received from *E. coli* grown in 2% glucose-supported M9 medium in the presence of 1 mM of $CoCl_2$).

It should be mentioned that the low molecular weight compounds found in ECMs by *approach 2* were mostly represented by derivatives of amines, sugars, carboxylic acids, free fatty acids (FFA) and glycerol. However, the exact type of signaling molecule (or group of
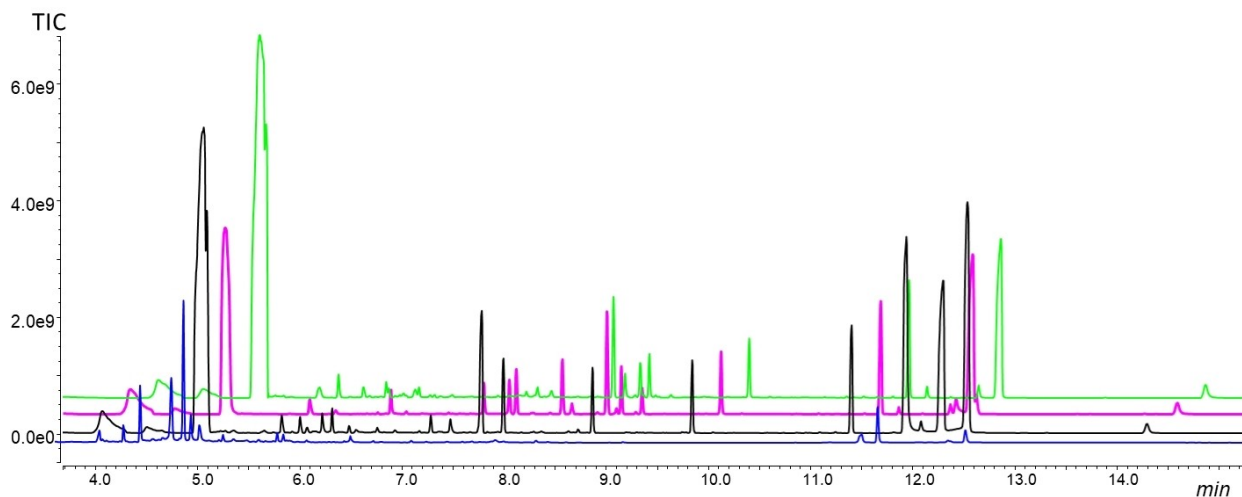

FIGURE 1 GC-MS chromatograms obtained from MXT column (cross-bond 100% dimethyl polysiloxane) for *E. coli* ECMs after derivatization with MSTFA (*approach 2*): blue – sample I; black – sample II; rose – sample III; green – sample IV.

molecules) which can be utilized for the electrochemical profiling of samples remains unclear (*see next section*).

3.3 | Determination and validation of the nature of the main signaling electroactive molecule in ECM of *E. coli*

Since GC-MS indicated wide spectra of analytes present/formed in *E. Coli* ECM the clarification of the chemical nature of the main electroactive components is necessary. Despite the richer chemical profile of sample IV as compared to sample I (Figure 2), most of the defined compounds by approach 2 were specified as non-electroactive at Pd-based electrodes [25–28, 29]. Based on the high oxidation potential a wide range of furanose and xylose derivatives formed in sample IV can be excluded from the list of potential electroactive candidates and possible signaling analytes for ECMs profiling [30, 31]. Free fatty acids (FFA) are also not electroactive on the non-enzymatic electrodes [32].

In sample I the defined low molecular weight compounds were ranged from 74.12 Da (1-dodecanol) to 358.57 Da (glycerol monostearate), see ESI, Table S1. However, within this list only glycerol as a small molecular weight compound (m/z 92.05) and its derivatives could readily be oxidized at various electrocatalysts and experimental conditions [33, 34]. In addition, quantitative yield (wt %) of glycerol was the highest in this list. Hence, glycerol could be considered as a potentially perspective signaling electroactive component.

The formation of glycerol and acetin (1,2,3-triacetylglycerol) marked as compounds **2** and **6** on the black chromatogram was confirmed only in sample I, see Figure 1 and Figure 2. The appearance of glycerol and its derivatives in this sample can be explained by the cleavage of triacylglycerides into glycerol and FFA [35, 36]. Interestingly, in addition to the formation of glycerol-related products in sample I a parallel decrease of FFA amount (see retention time, RT, between 12 and 14 min) was recorded, Figure 2, see also Figure 1.
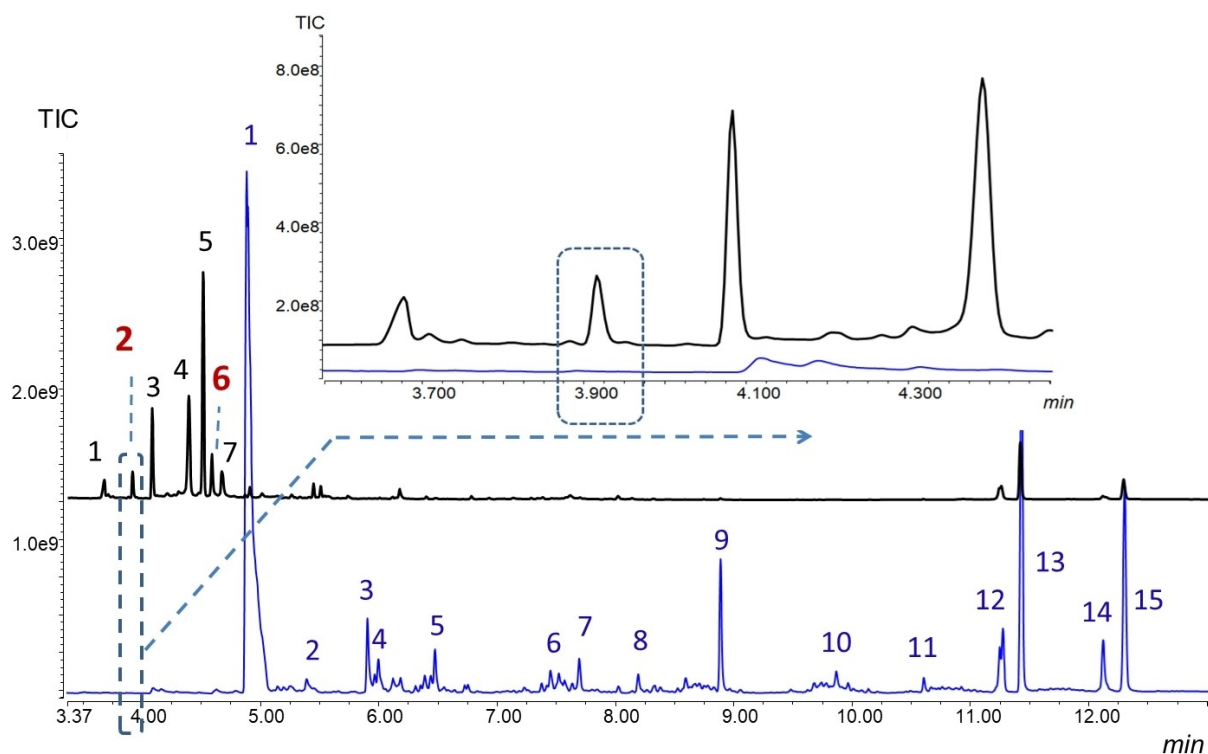

FIGURE 2 GC-MS chromatograms obtained for *E. coli* ECM after derivatization with MSTFA (*approach 2*); sample I (*black*): 1 – 2-butanoic acid, 3-methylester; 2 – glycerol, 2TMS; 3 – cyclotrisiloxane, hexamethyl; 4 – cyclotertasiloxane, octamethyl; 5 – 1-n-butoxy-1-methyl-1-silacyclohexane; 6 – acetin (1,2,3-triacetylglycerol); 7 – phenylmethyl sulfide; sample IV (*blue*): 1 – silanol-trimethyl phosphate 3:1; 2 – nonanoic acid, 3TMS derivative; 3 – butanoic acid 2-methyl-trimethylsiloxy trimethyl silylester; 4 – deoxypentofuranose; 5 – 1-dodecanol TMS derivative; 6 – dotricontane, 1-iodo; 7 – isopropyl myristate; 8 – 4-hydroxyphenyllactic acid 3TMS derivative; 9 – palmitic acid TMS derivative, 10 – stearic acid TMS derivative; 11 – 1-monomyristine 2TMS derivative; 12 – monopalmitin 2TMS derivative; 13 – stearic acid, TMS derivative; 14 – hexadecane, 2,6,10,14-tetramethyl stearic acid, TMS derivative; 15 – 2-glycerol monostearate, 2TMS. *Note:* small peaks in the blue chromatogram were attributed to pyranose, furanose and xylose derivatives (products of starch transformation by *E. coli*). *Insert – zoomed area of the chromatograms corresponding to glycerol.*

In contrast, for samples II–IV only FFA-corresponding peaks were detected in the chromatograms; the formation of glycerol and acetin in the ECMs of these samples was not confirmed by the *approach 2*, see Figure 1 and Figure 2. At the same time, the higher amount of phosphate salts and free fatty acids detected in samples II–IV could simply mask the signals raised from glycerol. To minimize the matrix effects, next, these samples were spiked by 100 mM of glycerol: the presence of glycerol-related peaks in this case was almost identical to sample I (shown for sample IV as a case study); at the same time, a clear decrease of matrix-related signals similar to the chemical profile recorded for sample I was detected (Figure 3). This simple experiment approves the absence of glycerol in samples II–IV and validates its presence in sample I. On the other side, it could be concluded that the presence of different carbon sources (e.g., glucose vs. starch) and the usage of additional chemicals in growth medium (H_2O_2 or $CoCl_2$) significantly affect the formation of glycerol in ECM of *E. coli*.

Notably, for the intact ECMs (without derivatization, *approach 1*) in the extraction ion mode (EIC) at the mass corresponding to glycerol at *m/z* 92 no evidence for its presence was obtained, ESI, Figure S6. It highlights the importance of a sample preparation step and the used GC-MS protocol (see results obtained by *approach 1 vs approach 2*) for the entire analytical merit of the assay.

FT-IR studies performed on the next step confirmed the above obtained GC-MS dependencies. Thus, exclusively glycerol-related compounds were seen in ECM of *E. coli* obtained during cells cultivation in glucose-supported M9 medium (sample I) *vs* samples received from the starch-supported medium (sample IV).

After spiking of sample I by 100 mM of glycerol its presence in this sample detected by FT-IR got more pronounced, ESI, Figure S7. More significantly, the total FT-IR chemical profile of sample I became identical to which was obtained for 100 mM of the individual glycerol diluted in glucose-supported M9 medium.

To sum it up, namely glycerol can be used as a characteristic signaling molecule to distinguish ECM of *E. coli* depending on the growth conditions of bacterial cells. Glycerol is an important compound participating in the lipid metabolism in cells; hence, its presence and concentration can readily be used as a marker of the cellular status depending on their growth conditions in the future.

3.4 | Pd-ink modified electrode activity to glycerol in model solutions

It should be mentioned, that glycerol electroanalysis is strongly affected by the electrocatalyst type, design of the sensing layer, media content and pH [37–39]. From the literature several electrocatalysts, *viz.* Pd-based electrodes can be used for an efficient glycerol electrooxidation [37–39]. However, due to the modified/changed structure, morphology and surface chemistry of Pd particles in the design of electrodes [40] the exact conditions of glycerol electrooxidation, *i.e.* polarization mode, electrolyte composition and pH should be defined/tuned separately for each type of the electrocatalytic layer.

From this point of view, the preliminary experiments of glycerol electrooxidation on Pd-ink modified electrode in model solutions of phosphate buffer at
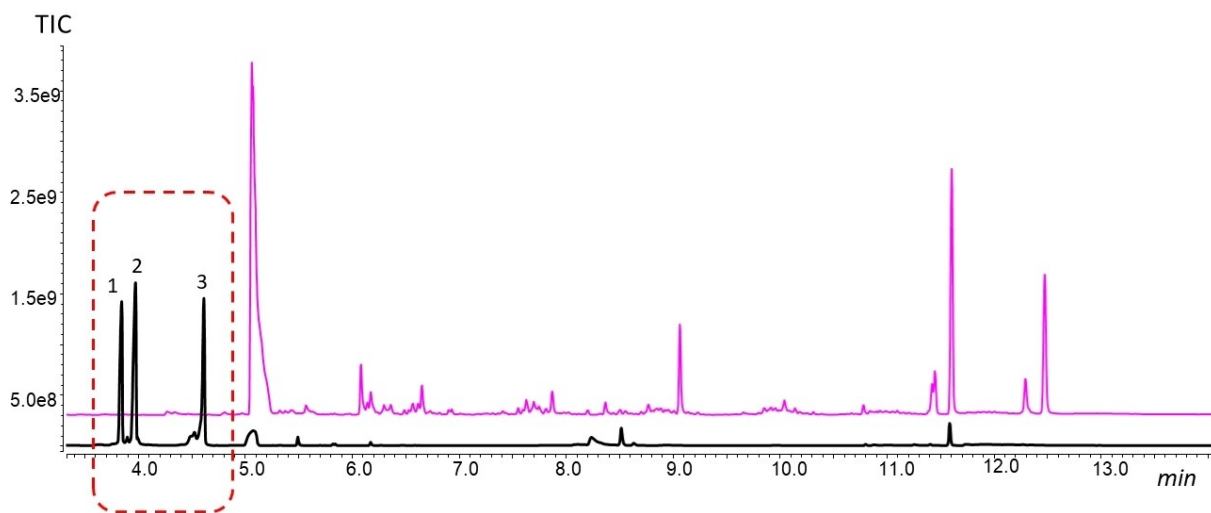

FIGURE 3 GC-MS chromatograms obtained on a MXT column by *approach 2* for sample IV after derivatization with MSTFA: (*rose*) – intact ECM obtained from sample IV (description of peaks is given in Figure 2); (*black*) – sample IV spiked by 100 mM glycerol: 1 – glycerol,1-tert-buthyl-3-methylsilyl ether; 2 – glycerol, 2 TMS; 3 – glycerol, 3 TMS.

pH 7 and potassium hydroxide at pH 12 with 100 mM of glycerol were carried out. As it is seen from Figure 4 the electrooxidation of glycerol at Pd-ink is superior in alkaline media. There are two anodic waves at −0.1 and 0.6 V corresponded to glycerol electrooxidation and the cathodic wave at −0.3 V with a compromise current between the cathodic reduction of Pd-surface oxides formed during the anodic scan and anodic glycerol electrooxidation. The latter compromise current is typical for Pd electrodes operated in alcohol alkaline solutions [11, 14]. The second anodic peak at a higher potential corresponded to glycerol oxidation on the oxidized Pd surfaces. The mechanism of glycerol oxidation on Pd-based electrodes was discussed in detail earlier [41, 42].

To summarize, Pd-ink modified electrode is electroactive to glycerol in alkaline media in a scan range from −0.4 V to 0.8 V. Hence, it is possible to propose an electrochemical protocol for a profiling of ECM of *E. coli* based on the target electroanalysis of this electroactive molecule in a complex fermentation medium. However, the matrix effects mentioned in the previous section for GC-MS analysis could also be significant in electrochemical tests. In this regard, the conditions of electrochemical profiling of glycerol in biological media should be optimized (*see next section*).

3.5 | Glycerol electrooxidation in fermentation media at Pd-ink modified electrodes

Firstly, the performance of Pd-ink modified electrode was studied in CV mode in a droplet of M9 medium at pH 7. Then the received signal at pH 7 was compared to the response obtained in the same medium at pH 12.

As it is seen from Figure 5, the electrochemical signal of Pd-ink modified electrode is almost absent in M9 medium at pH 7 and appears only at pH 12 as it was seen in model solutions, see Figure 4. Briefly, only two peaks were detected in CV plots. The wave with a high anodic current appears on the anodic branch of CVs with a peak potential at 0.6 V. The onset potential of this anodic current corresponds to the formation of PdO on the surface of Pd [14]. It means that the presence of the adsorbed oxygen on the Pd-surface facilitates the oxidation of glycerol even in a complex media (fermentation medium in this case). Another smaller peak on the cathodic branch of CV corresponds to electroreduction of the adsorbed oxygen formed on Pd during the anodic scan. The peak at −0.1 V corresponded to electrooxidation of glycerol on the reduced Pd surface in model solutions (Figure 4) is absent in M9 medium at pH 12 (Figure 5), most probably due to adsorption of non-electroactive components of media.
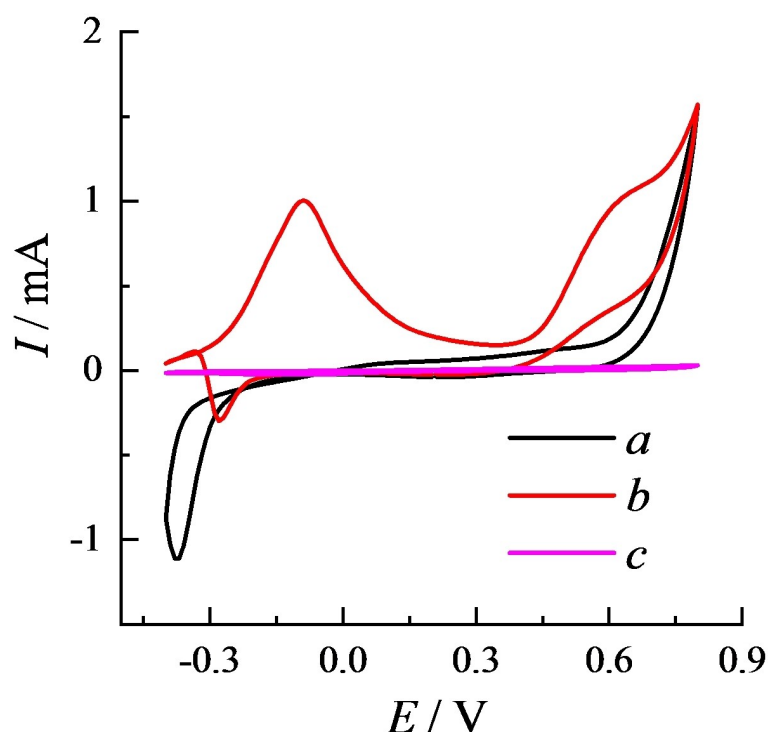

F I G U R E 4 CV plots recorded from Pd-ink modified SPE in (*a*) KOH, pH 12 solution and in 100 mM glycerol in model solutions (*b*) pH 12 and (*c*) pH 7.
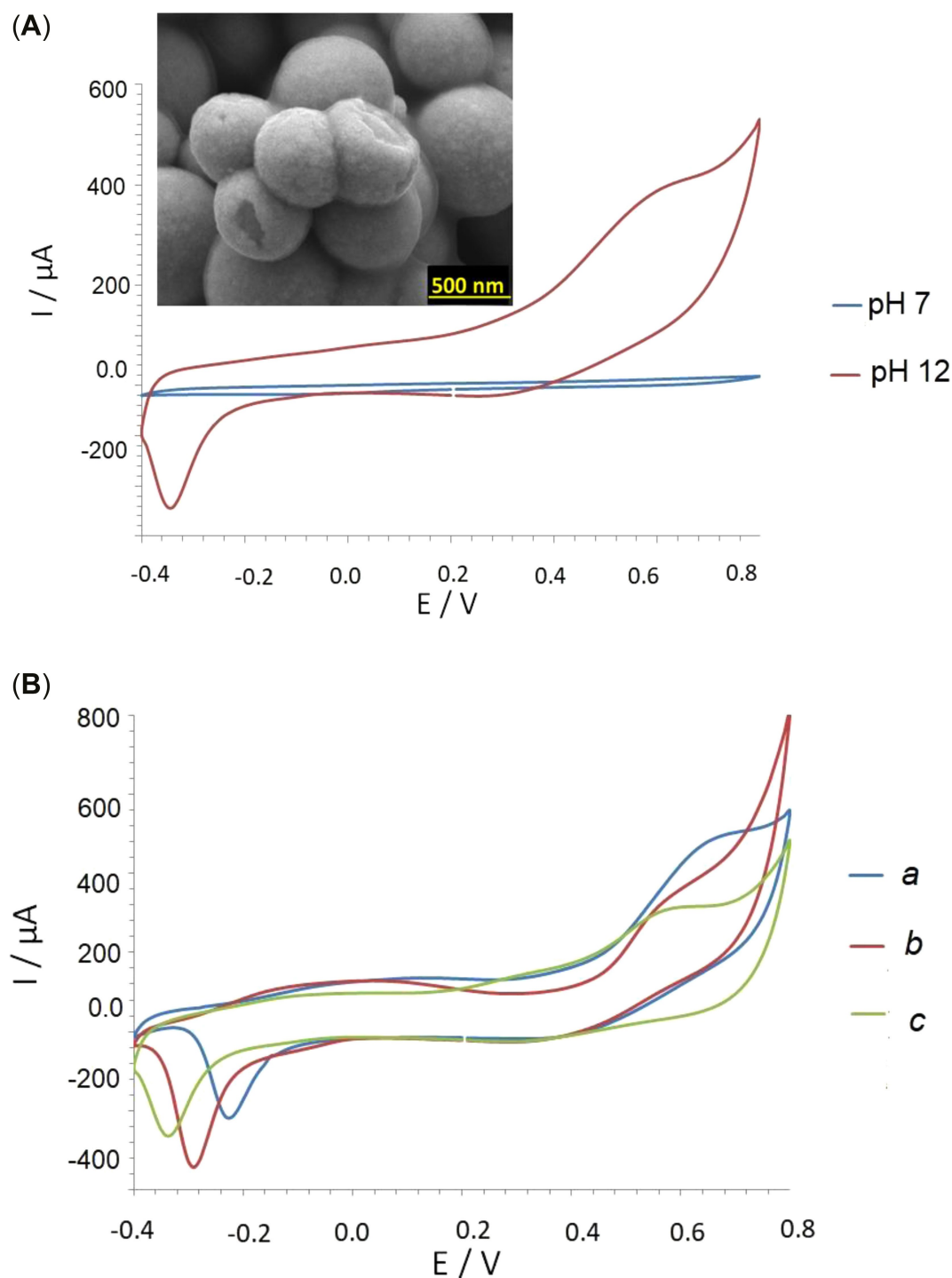
FIGURE 5 CV plots recorded from Pd-ink modified electrode at 20 mV/s: (A) in glucose-supported M9 medium with various pH. *Insert* – SEM image of Pd-ink modified SPE. (B) in various media with pH 12 ± 0.2: (*a*) – 100 mM of glycerol in M9 supported by 2% glucose; (*b*) – 100 mM of glycerol in M9 supported by 2% starch; (*c*) – 100 mM of glycerol in HC medium supported by 2% glucose.

Since glycerol oxidation occurs exclusively in alkaline solutions the establishment of the optimal pH value of media for the subsequent electrochemical procedure is important. As it is seen from Figure 6, the increase of pH of M9 medium spiked with 100 mM of glycerol from 7 to 12.4 leads to a current increase at 0.6 V. A further increase of pH to 13 or 13.5 was accompanied by a rapid diminution of the current response at 0.6 V due to alkaline hydrolysis of organic components in medium. The highest current was reached at pH 12.4. Nevertheless, in order to avoid the impact of hydrolysis processes on results and to simplify the experiments during glycerol detection in M9 a pH value of 12 was used.
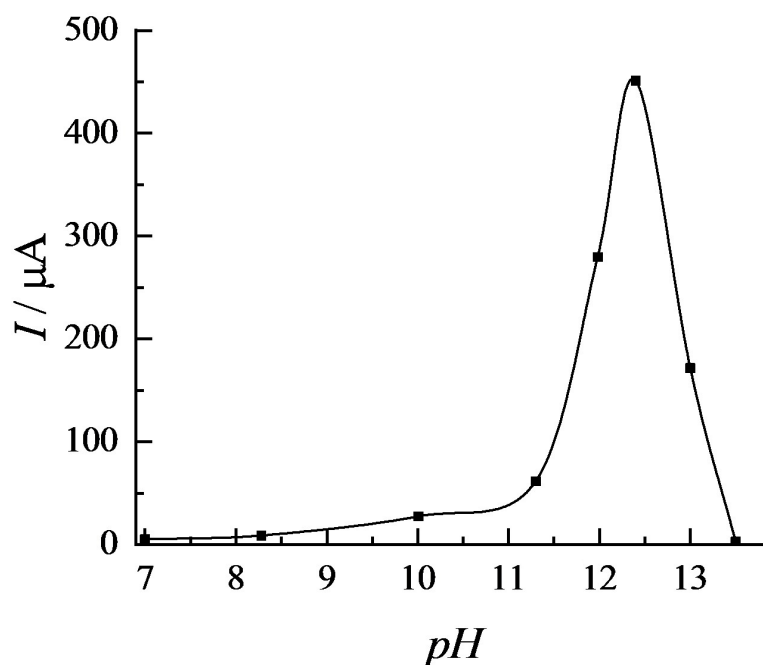
FIGURE 6 Impact of M9 medium pH spiked with 100 mM of glycerol on the current response at 0.6 V. *Note:* data were obtained at Pd-ink modified electrode at 20 mV/s.

It is important to note, that in glycerol containing solutions the anodic wave appears in all model media (M9 and HC at pH 12) independently on the nature of supported substrates (glucose or starch), Figure 5B. However, the peak shape, peak potential, position and peak current strongly depend on the composition of the analyzed solution. It also explains the shifting of the cathodic peak from −0.2 V to −0.38 V.

The observed electrochemical behavior of the Pd-ink-modified electrode in complex fermentation media highlights the ambiguous kinetic of the electrode processes on the one side and the complex adsorption nature of oxygen and glycerol on the other side. The highest current response at ~0.6 V corresponding to glycerol electro-oxidation on Pd-surface was observed in M9 glucose-supported medium, see Figure 5B, *curve a*. The dependencies of the anodic current on glycerol concentration in this M9 medium at pH 12 as well as in starch-supported M9 medium are summarized in ESI, Figure S8. The linear detection range (LDR) established for glycerol in glucose-supported M9 medium on Pd-ink modified SPEs at 0.6 V was from 1 to 150 mM and from 5 mM to 250 mM in starch-supported medium, respectively, demonstrating that, the proposed electrochemical system could be used for a rapid and reliable glycerol quantification in *E. coli* ECMs (see also *section 3.6*).

3.6 | A rapid electrochemical profiling of *E. coli* ECM via monitoring of glycerol by Pd-ink modified electrode

Indeed, the change of acidity of samples from the physiological value of 7 to basic pH 12 allowed the visualization of glycerol in ECM obtained from cells grown in glucose-supported M9 medium, Figure 7 (shown for sample I, glucose-supported M9 medium). In sample I the presence of glycerol was previously approved by GC-MS and FT-IR, see *sections 3.1 and 3.2*. Notably, that the form of CV plot recorded for glycerol standard diluted in glucose-supported M9 medium and the peak maximum in the anodic range were very similar to the CV curve obtained for the sample I (Figure 7A).

In contrast, CV plots recorded in a droplet of ECM received from cells grown in starch-supported M9 medium (sample IV) did not exhibit the characteristic peak at ~0.60–0.63 V that could be assigned to glycerol oxidation at a Pd-ink modified electrode, Figure 7B, see *line a*. At the same time after addition of glycerol standard (spiking of 100 mM glycerol in sample IV) or ESTD (glycerol prepared in the same starch-supported medium) the presence of glycerol and its electro-oxidation at the anodic range at the same electrode and experimental conditions used was obvious, Figure 7B,
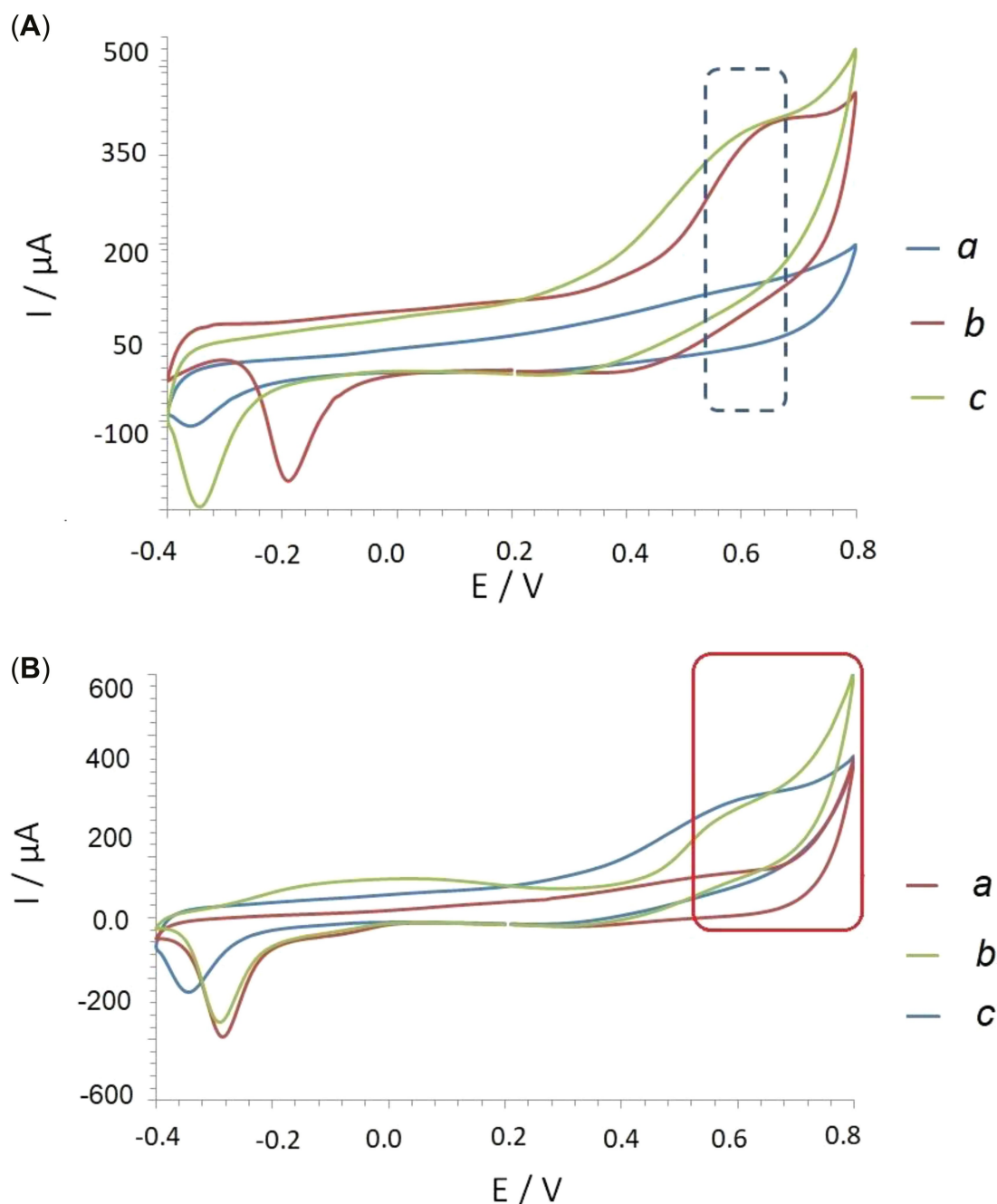
FIGURE 7 (A) CV plots recorded from Pd-ink modified electrode at 20 mV/s in a droplet of: *a* – M9 medium, pH 12.3; *b* – *E. coli* ECM, cells cultivated in glucose supported M9 medium (sample I), pH 11.98; *c* – 100 mM glycerol in M9 medium (ESTD), pH 11.95. (B) – CV plots recorded in a droplet of: *a* – ECM obtained from *E. coli* grown in starch supported M9 (sample IV), pH 12.0; *b* – same sample spiked by 100 mM of glycerol (standard addition), pH 12.0; *c* – 100 mM glycerol in starch-supported M9 medium (external standard, ESTD), pH 11.80.

see *lines b,c.* In other words, in the case of glycerol formation in ECM samples its presence can rapidly be visualized/recognized at Pd-ink modified electrodes at pH 12 regardless of the carbon source used (*i.e.* glucose or starch).

The obtained electrochemical dependencies were in line with results of GC-MS analysis of ECMs. Thus, no glycerol was detected in chromatograms of samples II–

IV by GC-MS (*approach 2*) and no characteristic peak of glycerol electrooxidation was recorded for these samples at Pd-ink modified electrode at pH 12, Figure 8A. However, the subsequent spiking of 100 mM glycerol in samples received after $CoCl_2$ (sample II) and H_2O_2 (sample III) treatment clearly indicated the exact added amount of glycerol, Figure 8B. More interestingly, the peak potential and its current intensity for sample II and sample
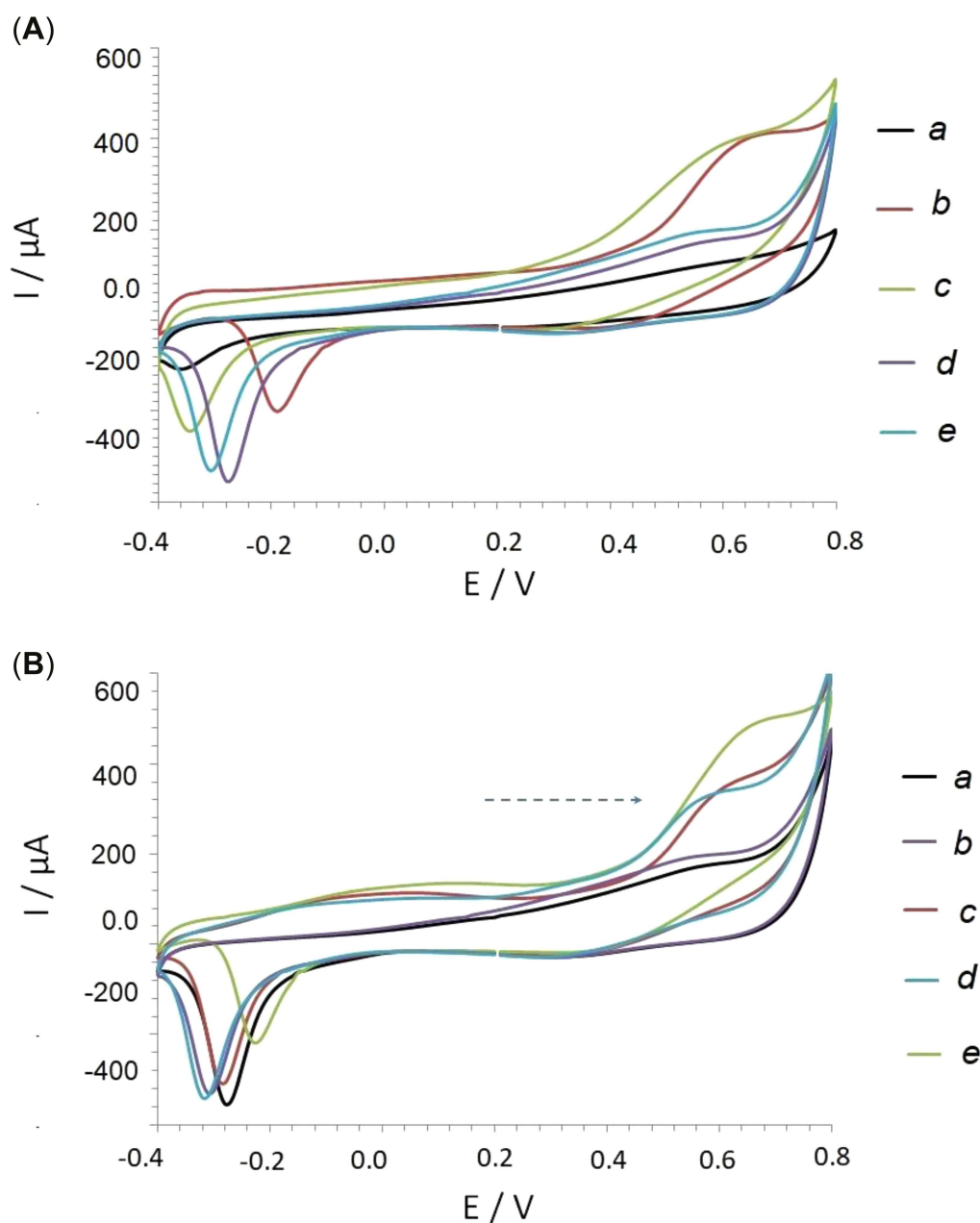
FIGURE 8 (A) CV plots recorded from Pd-ink modified electrode at 20 mV/s in a droplet of: *a* – glucose-supported M9 medium. *b* – *E. coli* ECM, cells grown in medium (a), sample I. *c* – 100 mM of glycerol standard in medium (a). *d* – *E. coli* ECM, cells were grown in the presence of 1 mM of H_2O_2 (sample III). d – *E. coli* ECM, cells were grown in the presence of 1 mM of $CoCl_2$ (sample II). (B): *a* – *E. coli* ECM, cells grown in the presence of 1 mM of H_2O_2 (sample III). *b* – *E. coli* ECM, cells were grown in the presence of 1 mM of $CoCl_2$ (sample II). *c* – sample III spiked with 100 mM of glycerol. *d* – sample II spiked with 100 mM of glycerol. *e* – sample I spiked with 100 mM of glycerol; cells were grown in M9 medium without any chemical addition. *Note:* in all samples M9 medium was supported by 2 % glucose. pH of all samples was set to 12 ± 0.2.

III completely coincided at 0.6 V after addition of glycerol. This highlights the equal absence of glycerol in these two samples from the one side and the accuracy of glycerol electrodetection at Pd-ink modified SPE and used conditions on the other side. Qualitative comparison of the obtained results by CV and GC-MS assays indicating the presence/absence of glycerol in tested samples depending on the used cultivation conditions is summarized in Table 1.

The biological significance of the obtained results is in the possible pre-conclusion that despite the usage of glucose applied as a carbon source, *E. coli* cannot efficiently decompose FFA to glycerol under external stress conditions, *viz.* chemicals loading ($CoCl_2$, H_2O_2).

T A B L E 1   – Qualitative comparison of GC-MS and CV-profiling of ECM of *E.coli* using glycerol as a signaling molecule.

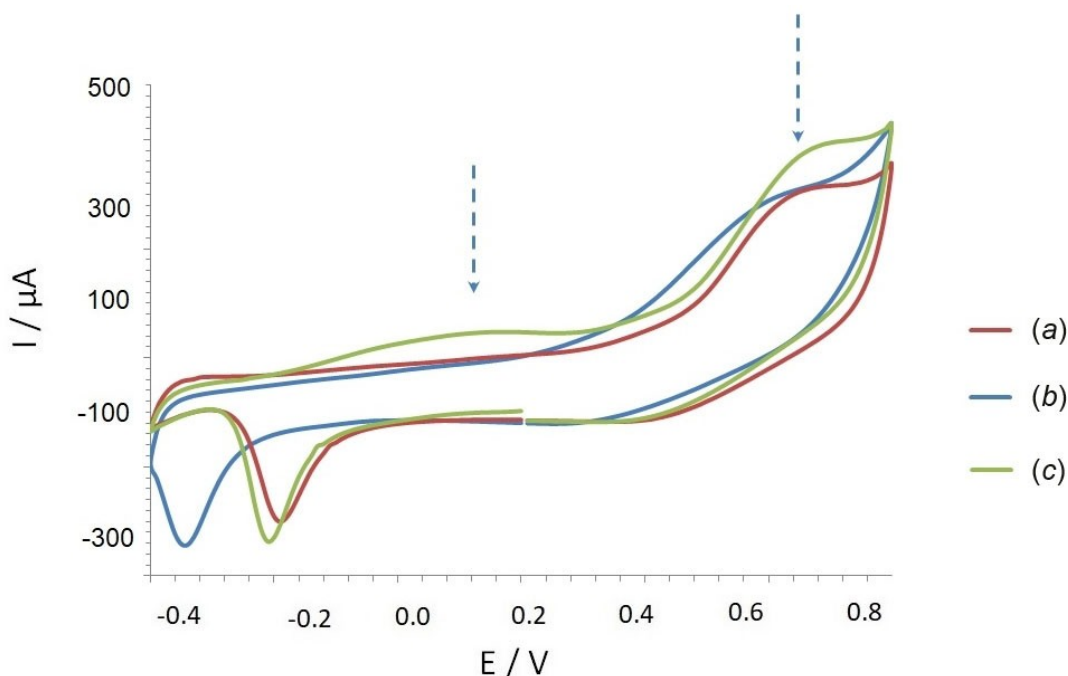|	Presence of glycerol	
Sample	**GC-MS**	**CV-analysis by Pd-ink modified electrode**
M9 medium*	–	–
M9 medium + 100 mM glycerol	+	+
Sample I	+	+
Sample I + 100 mM glycerol	+	+
Samples II–IV	–	–
Samples II–IV + 100 mM glycerol	+	+

*M9 was supported by 2 % glucose.

F I G U R E 9   CV curves recorded from Pd-ink modified electrode at 20 mV/s in a droplet of fermentation probes: (*a*) – sample I; (*b*) – 100 mM glycerol in 2 % glucose-supported M9 medium; (*c*) – sample I spiked by 100 mM of glycerol. pH was in the range of 12 ± 0.2.

3.7 | Some features of glycerol quantification by Pd-ink modified electrode in complex fermentation media

With regards to the quantitative analysis of glycerol in fermentation media, it should be highlighted that the use of GC-MS for this goal is not a trivial task. Thus, instead of a single and intensive peak on the chromatogram corresponding to glycerol standard three peaks related to its derivatives, *viz.* glycerol, 2 TMS-1-tert-buthyl-3-methylsilyl ether glycerol and 3 TMS glycerol were observed, see Figure 3, *black line*. The similar trend was detected for real ECM sample containing glycerol, see Figure 2, *black line.* Remarkably, the spiking of ECMs containing glycerol by additional amount of glycerol in

the concentration level of 50–100 mM also led to the appearance of the novel low-potential anodic peak in CV plot at approx. ~0.1 V. This peak corresponds to glycerol electrooxidation at a low potential (Figure 9) was previously obtained in model solution (Figure 4) and corresponded to oxidation of alcohol on the reduced Pd surface [11, 27]. In other words, glycerol oxidation at Pd-ink modified SPEs at pH 12 could be affected by the concentration of glycerol (*i*) and type of the used matrix/media (*ii*).

The subsequent CV experiment carried out in model solutions containing 100 mM of glycerol confirmed this assumption. Thus, this low-potential anodic peak got more pronounced at pH 12 in DI water at 100 mM of glycerol, see Figure 4b. In addition, this peak seen in M9

medium at approx. ~0.1 V in model solutions was shifted to a more cathodic range, *i.e.* −0.1 V (Figure 4) caused by absence of matrix effects [43].

From the analytical point of view the obtained data indicate the impossibility of multiple standard addition approach for quantitative analysis of *E. coli* ECMs. Thus, with increase of spiking concentration the intensity of the second peak at 0.1 V increased while the signal at 0.6 V decreased, see also ESI, Figure S8. However, the quantification of glycerol in *E. coli* ECMs by ESTD approach allowing visualizing of glycerol as a single and intensive peak at 0.6 V appeared to be possible. Selected data assay for glycerol electroanalysis by ESTD in *E. coli* ECMs are summarized in Table 2.

Interestingly, the increase of cultivation time for the sample I from 24 h to 48 h led to a decrease of the glycerol concentration from 67.14 mM to 17.4 mM, respectively. No glycerol in sample I was found in case of a further increase of the cultivation time to 72 h and 96 h.

The obtained results were in line with a life cycle of *E. coli* [44–47]. Thus, in the lack of a carbon source (glucose as a case study, sample I) in a medium as a result of an increase of cultivation time from the one side and the formation of glycerol from triacylglycerides [35, 36] on the other side might cause the switching of cellular metabolism [44–47]. During this process the formed glycerol in sample I will be consumed by cells supporting their survival in the lack of a carbon source.

3.8 | Towards target electroanalysis of signaling analytes in bacterial ECM

The comparison of the electrochemical approach used for the profiling of *E. coli* ECM with the conventional GC-MS assay indicates that each approach individually has disadvantages and limitations, but their combination leads to the success (Table 3). In other words, only by

TABLE 2 – Assay data for glycerol electroanalysis by ESTD in *E.coli* ECM* using Pd-ink modified electrode.

Sample**	Electrochemical assay utilizing Pd-ink modified electrode			Glycerol concentration, mM	R^2
	Response, µA	Recovery***, %	Error, %		
	2% glucose-supported M9 medium			$y = 0.7 \cdot x + 318$	
Sample I	365 ± 5	102 ± 2	8	67.14 ± 5	
Sample II	200 ± 7			Not found	0.998
Sample III	179 ± 9			Not found	
2% starch-supported M9 medium				$y = 0.152 \cdot x + 239.56$	0.995
Sample IV	190 ± 10	99 ± 3	2	Not found	

*evaluated at Pd-ink modified electrode at 0.6 V;
**cells cultivated for 24 h;
***evaluated by spiking of 100 mM glycerol. The recovery was evaluated according to [48].

TABLE 3 – A comparative table of assays employed for profiling of *E. coli* ECM.

Parameter	GC-MS	Electrochemical approach (CV)
Qualitative initial information about the type of electroactive compounds present in ECM	yes	no
Possibility for qualitative analysis of the target electroactive signaling analyte	yes	yes
Qualitative analysis based on the single peak	no*	yes
Sample destructive or not	invasive	non-invasive
Duration of analysis	40 min	3–4 min
Sample derivatization	required	not required
Data acquisition	complex and time consuming	simple and rapid
Cost and chemicals effectiveness	no	yes
Portativity	no	yes

*glycerol is visualized in chromatogram as three peaks, i.e. glycerol,1-tert-buthyl-3-methylsilyl ether; glycerol, 2 TMS and glycerol, 3 TMS, see Figure 3.

optimization and combination of GC-MS and CV protocols it is possible to conduct the electrochemical profiling of bacterial ECM (*E. coli* as a case study) used as a source of electroactive low molecular weight compounds.

It should also be stressed that the replacement of Pd-ink SPE used in this work as a case study by other functional layers or change of electrochemical conditions (pH, scan window, etc.) could lead to the extension of capabilities of electrochemical profiling of ECM, *i.e..* by detection and electroanalysis of different signaling electroactive compounds or metabolites present in the sample (see Table S1, ESI). For this goal, the provided protocol could serve as a specific guideline for determination, validation and analysis of these signaling electroactive compounds in complex biological samples, *viz.* bacterial ECM.

4 | CONCLUSIONS

In this work for the first time the electrochemical profiling of *E. coli* ECM was conducted. Primary, by means of gas chromatography mass spectrometry (GC-MS) the nature of a signaling electroactive compound (glycerol) formed in *E. coli* ECM as a result of bacterial activity was revealed. The obtained knowledge was used for the optimization of an electroanalytical protocol utilizing cyclic voltammetry (CV) for glycerol detection in complex *E. coli* ECM.

In contrast to GC-MS assay based on the obligatory derivatization stage, the electrochemical approach utilizing commercial Pd-ink modified screen printed electrodes (SPEs) provides a rapid data acquisition, simplicity of analysis at reasonable costs and requires only a minimal amount of sample preparation, *i.e.* cells centrifugation from ECMs.

The obtained data could be considered as a first step towards interaction studies between small molecular weight compounds of *E. coli* ECM with SPEs that could unlock the possibility of using of electroanalytical approaches for a non-destructive *in vitro* profiling of cells.

AUTHOR CONTRIBUTIONS

Y. E. Silina: conceptualization, data analysis, validation, project administration, funding acquisition, wrote the original draft; *E. V. Zolotukhina*: data analysis, validation, reviewing and editing of the manuscript; *M. Koch*: formal analysis, reviewing and editing of the manuscript; *C. Fink-Straube*: formal analysis, reviewing the manuscript.

CONFLICT OF INTEREST STATEMENT
The authors declare that they have no known competing financial interests or personal relationships that could have appeared to influence the work reported in this paper.

DATA AVAILABILITY STATEMENT
The data that support the findings of this study are available from the corresponding author upon reasonable request.

REFERENCES
1. D. A. Hufnagel, W. H. Depas, M. R. Chapman, *Microbiol. Spectrum* **2015**, *3*, 3.3.23.
2. S. Balasubramanian, K. Yu, D. V. Cardenas, et al., *ACS Synth. Biol.* **2021**, *10*, 2997–3008.
3. C. Hung, Y. Zhou, J. S. Pinkner, et al., *mBio.* **2013**, *4*, e00645-13.
4. J. K. Kular, S. Basu, R. I. Sharma, *J. Tissue Eng.* **2014**, *5*.
5. D. P. Clark, *FEMS Microbiol. Rev.* **1989**, *5*, 223–234.
6. J. M. Cevallos-Cevallos, M. D. Danyluk, J. I. Reyes-De-Corcuera, *J. Food Sci.* **2011**, *76*, 238–246.
7. C. Zscheppank, H. L. Wiegand, C. Lenzen, et al., *Anal. Bioanal.* **2014**, *406*, 6617–6628.
8. H.-H. Chiu, C.-H. Kuo, *J. Food Drug Anal.* **2020**, *28*, 60–73.
9. F. K Choudhury, P. Pandey, R. Meitei, et al., GC-MS/MS Profiling of Plant Metabolites, **2022**, Methods in molecular biology (Clifton, NJ) 2396, pp. 101–115.
10. M. Meyer, L. Montero, S. W. Meckelmann, O. J. Schmitz, *Anal. Bioanal.* **2022**, *414*, 2117–2130. <
11. S. A. Kleinikova, M. G. Levchenko, A. B. Yalmaev, et al., *Electrochim. Acta* **2022**, *409*, 139998.
12. S. S. Mahapatra, J. Datta, *Int. J. Electrochem.* **2011**, *2011*, 1–16. https://doi.org/10.4061/2011/563495.
13. S. A. Kleinikova, K. V. Gor'kov, E. V. Gerasimova, et al., *Electrochim. Acta.* **2021**, *377*, 138076.
14. K. V. Gor'kov, N. V. Talagaeva, S. A. Kleinikova, et al., *Electrochim. Acta.* **2020**, *345*, 136164.
15. J. T. C. Barragan, S. J. Kogikoski, E. T. S. G. da Silva, L. T. Kubota, *Anal. Chem.* **2018**, *90*, 3357–3365.
16. K. M. Hassan, Z. Khalifa, G. M. Elhaddad, M. Abdel Azzem, *Electrochim. Acta* **2020**, *355*, 136781.
17. D. Basu, S. Basu, *Int. J. Hydrogen* **2012**, *37*, 4678–4684.
18. N. Hirose, I. Kazama, R. Sato, et al., *J. Biosci. Bioeng.* **2021**, *132*, 519–523.
19. J. J. White, N. Cain, C. E. French, *bioRxiv* **2019**, 841023.
20. L. M. Rosales-Colunga, A. Martínez-Antonio, *Microb. Cell Fact.* **2014**, *13*, 74.

21. W. Terakosolphan, A. Altharawi, A. Poonprasartporn, et al., *Int. J. Pharm.* **2021**, *609*, 121118.

22. A. Mona, K. Roselina, R. R. Abdul, et al., *Czech J. Food Sci.* **2018**, *36*, 403–409.

23. J. Rohloff, *Molecules* **2015**, *20*, 3431–3462.

24. Y. E. Silina, C. Fink-Straube, M. Koch, E. V. Zolotukhina, *Bioelectrochemistry* **2023**, *149*, 108283.

25. T.-J. Wang, F.-M. Li, H. Huang, et al., *Adv. Funct. Mater.* **2020**, *30*, 2000534.

26. P. J. Kulesza, S. Pieta, I. A Rutkowska, et al., *Electrochim. Acta* **2013**, *110*, 474–483.

27. C. Xu, L. Cheng, P. Shen, Y. Liu, *Electrochem. Commun.* **2007**, *9*, 997–1001.

28. J. Torrero, Á. García, M. Retuerto, et al., *J. Electroanal. Chem.* **2022**, *908*, 115968.

29. C. Sandford, M. A. Edwards, K. J. Klunder, et al., *Chem. Sci.* **2019**, *10*, 6404–6422.

30. T. Rafaïdeen, S. Baranton, C. Coutanceau, *Appl. Catal. B* **2019**, *243*, 641–656.

31. A. T. Governo, L. Proença, P. Parpot, et al., *Electrochim. Acta.* **2004**, *49*, 1535–1545.

32. J. Kang, A. T. Hussain, M. Catt, et al., *Sens. Actuators B* **2014**, *190*, 535–541.

33. L. S. Oh, J. Han, E. Lim, et al., *Catalysts.* **2023**, *13(5)*, 892.

34. E. C. dos Santos, R. B. Araujo, M. Valter, et al., *Electrochim. Acta* **2021**, *398*, 139283.

35. R. M. Lennen, B. F. Pfleger, *Trends Biotechnol.* **2012**, *30*, 659–667.

36. H. J. Janßen, A. Steinbüchel, *Biotechnol. Biofuels.* **2014**, *7*, 7.

37. R. Ivanov, A. Nakova, V. Tsakova, *Electrochim. Acta.* **2022**, *427*, 140871.

38. N. Arjona, S. Rivas, L. Álvarez-Contreras, et al., *New J. Chem.* **2017**, *41*, 1854–1863.

39. A. Zalineeva, A. Serov, M. Padilla, et al., *J. Am. Chem. Soc.* **2014**, *136*, 3937–3945.

40. E. V. Zolotukhina, E. V. Butyrskaya, M. Koch, et al., *Phys. Chem. Chem. Phys.* **2023**, *25*, 9881–9893.

41. Li, D. A. Harrington, *ChemSusChem.* **2021**, *14*, 1472.

42. W. Y. Zhang, X. Y. Ma, S. Z. Zou, W. B. Cai, *J. Electrochem.* **2021**, *27*, 233–256.

43. W. Zhou, S. Yang, P. G. Wang, *Bioanalysis* **2017**, *9*, 1839–1844.

44. R. Yao, D. Xiong, H. Hu, et al., *Biotechnol. Biofuels* **2016**, *9*, 175.

45. M. S. Roman, A. Wagner, *PLoS Comput. Biol.* **2020**, *16*, 1–21.

46. E. Biselli, S. J. Schink, U. Gerland, *Mol. Syst. Biol.* **2020**, *16*, e9478.

47. K. Martínez-Gómez, N. Flores, H. M. Castañeda, et al., *Microb. Cell Fact.* **2012**, *11*, 46.

48. L. C. Rodríguez, A. M. Campaña García, F. A. Barrero, C. J. Linares, M. R. Ceba, *J. AOAC Int.* **1995**, *78*, 471–476.